

Original Article

Hidden gems of the abyss: first species of azooxanthellate scleractinian coral (Scleractinia: Deltocyathidae) attached to polymetallic nodules in the eastern Pacific Ocean

Guadalupe Bribiesca-Contreras^{1,2,†,*}, Nadia Santodomingo^{2,3,†}, Marcelo V. Kitahara^{4,5}, Erik Simon-Lledó⁶, Bethany F.M. Fleming^{1,7}, Thomas G. Dahlgren^{8,9}, Daniel O.B. Jones¹, Helena Wiklund⁸, Adrian G. Glover²

¹Marine Science, National Oceanography Centre, Southampton SO15 3ZH, United Kingdom

²Research, Natural History Museum, London SW7 5BD, United Kingdom

³Division of Marine Zoology, Senckenberg Research Institute and Natural History Museum, Frankfurt 60325, Germany

⁴Centre for Marine Biology, University of São Paulo, São Sebastião 11600-000, Brazil

⁵Department of Invertebrate Zoology, Smithsonian Institution, Washington, DC 20560, United States

⁶Institut de Ciències del Mar, ICM-CSIC, Barcelona 08003, Spain

⁷School of Ocean and Earth Science, University of Southampton, Southampton SO14 3ZH, United Kingdom

⁸Department of Marine Sciences, University of Gothenburg, Gothenburg 413 90, Sweden

⁹Division of Climate and Environment, NORCE Norwegian Research Centre, Bergen 5008, Norway

*Corresponding author. National Oceanography Centre, European Way, Southampton SO15 3ZH, United Kingdom. E-mail: guadalupe.bribiesca.contreras@noc.ac.uk

†Authors contributed equally.

ABSTRACT

Species in the genus *Deltocyathus* occur in every ocean basin except the Arctic and around Antarctica. They are most commonly found within 200 to 1000 m depth, with the deepest recorded species, *Deltocyathus parvulus*, found at 5080 m deep. Most *Deltocyathus* species are free-living, except for the Atlantic species *Deltocyathus halianthus*. Using an integrative taxonomic approach, here we describe *Deltocyathus zoemetallicus* sp. nov., collected at abyssal depths in the Clarion-Clipperton Zone and with a distribution spanning around 1000 km. This region of the central Pacific contains abundant mineral accretions known as polymetallic nodules that provide a significant source of hard substrate for sessile fixed species, including the species described herein. Seabed imagery transects on nodule fields were used to estimate standing stocks, with higher densities found in areas characterized by small nodules that almost completely cover the seafloor. These findings suggest that the abundance of *D. zoemetallicus* might depend on the density of polymetallic nodules. Consequently, despite its broad geographic range that may confer resilience at a large scale, this new coral species could be locally vulnerable to potential deep-sea mining activities.

Keywords polymetallic nodules; Scleractinia; deep-sea mining; phylogenetics; nodule-dwelling fauna; standing stocks

INTRODUCTION

Located between Hawai'i and Mexico, the Clarion-Clipperton Zone (CCZ) is a vast abyssal area of approximately 6 million km² (Wedding *et al.* 2013) and depths ranging from about 4000 m in the east to more than 5000 m in the west (Washburn *et al.* 2021). It is characterized by topographic features including seamounts,

hills, troughs, abyssal plains, and fracture zones (Kaiser *et al.* 2017). The occurrence of polymetallic nodules in the CCZ has led to increased exploration during the past decades. These mineral accretions contain valuable metals such as nickel, cobalt, and copper, and, therefore, have been targeted for commercial extraction (Hein *et al.* 2020). The CCZ is located beyond national

jurisdictions, and thus it is managed by the International Seabed Authority (ISA). To date, the ISA has granted 17 exploration licenses but the regulatory framework for exploitation of polymetallic nodules is still under development (International Seabed Authority 2024).

Recent studies have focused on characterizing the mega- (e.g. Molodtsova and Opresko 2017, Kersken *et al.* 2018a, b) and macrofaunal components (e.g. Bitner *et al.* 2013, Cairns 2016, Grischenko *et al.* 2018, 2024, Lim *et al.* 2024) of nodule-dwelling fauna. Despite these efforts, the diversity of these faunal components is still poorly understood, and dozens of species remain undescribed (Rabone *et al.* 2023). Sponges, octocorals, and bryozoans are commonly attached to polymetallic nodules (Amon *et al.* 2016, Simon-Lledó *et al.* 2023b); a life-habit recently associated with more constrained dispersal patterns (Simon-Lledó *et al.* 2025). However, there are to date no records of azooxanthellate scleractinian corals attached to them. For the CCZ, the only azooxanthellate coral that has been recorded is the free-living *Fungiacyathus* (*Fungiacyathus*) *cf. fragilis* Sars, 1872 (Bribiesca-Contreras *et al.* 2022). In recent expeditions to the CCZ, a few cup corals, all belonging to the same species, were found living attached to nodules. These specimens represent a new species within the genus *Deltocyathus* Milne Edwards & Haime, 1848.

The genus *Deltocyathus* comprises 26 extant species (Hoeksema and Cairns 2025) that have been found in every ocean basin except the Arctic and around Antarctica (Kitahara and Cairns 2021). Most species live within a depth range of 200 to 1000 m depth, but the deepest species, *Deltocyathus parvulus* Keller, 1982, has been found as deep as 5080 m (Kitahara and Cairns 2021). Most *Deltocyathus* species are free-living, except for the Atlantic *Deltocyathus halianthus* (Lindström, 1877).

Here, we describe the first species of azooxanthellate coral attached to polymetallic nodules using an integrative taxonomic approach. Additionally, we estimate the species densities using data from a remotely operated vehicle (ROV) seabed imagery survey.

MATERIALS AND METHODS

Collection, morphological analyses, and deposition of specimens

Specimens were collected during multiple cruises to the CCZ (Table 1, Fig. 1). Most specimens were recovered using an USNEL-type box corer to take sediment samples. Opportunistic samples were also taken from cores taken with a multicore OKTOPUS MC20 that was used for sampling meiofauna. Upon recovery of the gear, all nodules were carefully examined for any attached fauna. Nodules with fauna were placed in cold filtered sea water (CFSW) and transferred to the laboratory at-sea for further processing. Box core processing and data collection at-sea followed established DNA-taxonomy protocols (Glover *et al.* 2015). Specimens were photographed both attached to the nodule and detached, then placed in 80% or 90% non-denatured ethanol and shipped to the Natural History Museum (NHMUK), London, for further analyses.

In the laboratory, specimens were examined using stereomicroscopes and photographs of each were taken before and after DNA extraction. High-resolution imaging was conducted for three

specimens (NHMUK 2025.1, 2025.2, 2025.3) using a JEOL JSM IT500 scanning electron microscope (SEM) at the NHMUK. The corallites were not bleached, but soft tissue was removed during DNA extraction, then rinsed with distilled water and air dried. An FEI Quanta 650 FEG SEM (NHMUK) was used for one juvenile specimen (NHMUK 2025.5) following DNA extraction, distilled water rinsing, air drying, and gold coating. Additionally, micro-computed tomography (μ CT) imaging was conducted for the holotype (NHMUK 2025.1) using a Carl Zeiss Xradia Versa 520 μ CT scanner (NHMUK). Acquired images of dry specimens were imported, stacked, and rendered to create a 3D model using 3D Slicer 5.8.1 (Fedorov *et al.* 2012) and MeshLab 2023.12 (Cignoni *et al.* 2008). Identification and description followed Cairns (2000) and Kitahara and Cairns (2009). Vouchers and type material have been deposited at the Natural History Museum, London (NHMUK). Character abbreviations: calicular diameter (CD); great calicular diameter (GCD); height (H); pedicel diameter (PD); cycles of septa (S); and paliform lobe (P).

Seabed imagery

Faunal annotations of the imagery from the 2021 survey to NORI-D were used to estimate abundances (Supporting Information, Tables S1, S2). A total of fifteen 2 km-long photo transects were conducted across three study areas (MIN, Mining Area; CTA, Collector Test Area; PRZ, Preservation Reference Zone). Downward facing photos of the seafloor were collected with a Rayfin Benthic 6000 m camera (SubC imaging, resolution: 5344 × 4016 pixels) mounted on an ROV. The camera settings were shutter speed = 1/250 s, ISO = 100, aperture = F2.2, and focus MF = 0.2. The ROV flew at a speed of 0.1 m/s and a target altitude of 0.6–1.0 m with photographs collected every 9 s. Images were scaled using lasers set 10 cm apart. A total of 22500 non-overlapping images were collected, 12668 of which were annotated for fauna in BIIGLE 2.0 using the Abyssal Pacific Seafloor Megafauna Atlas (Simon-Lledó *et al.* 2023a). Due to the photographs being taken closer to the seabed than in other surveys in the area, it was possible to recognize the morphologic diagnostic characters to identify the *Deltocyathus* species. To avoid overestimating abundances by including similar organisms of other species, we excluded from the analyses all those specimens with a calicular diameter (CD) < 2.5 mm, retaining only very clear identifications. From the collected material, the smallest specimens were just over 1 mm in CD, but these could easily be confused with other species (e.g. bryozoans) when seen from seabed images. We acknowledge that this method could potentially underestimate the abundances, but it also increases the certainty of the identifications in the dataset.

DNA extraction, amplification, and sequencing

DNA was extracted using a DNeasy Blood & Tissue Kit (QIAGEN) or QuickExtract (Lucigen) following the manufacturer's instructions. Specimens were placed whole for digestion and recovered after 2 hours of incubation with tissue lysis buffer (ATL) + Proteinase K, in the case of QIAGEN kit, and rinsed with PCR-grade water. DNA was resuspended in 70 μ l of elution buffer (AE) buffer. Specimens placed in QuickExtract (20 μ l) were only left for 15 minutes for the first incubation at 65°C, then recovered and rinsed in deionized water after the second and final incubation. Digestion of soft tissue using ATL + Proteinase K slightly

Table 1. Details of number of specimens collected per cruise, with details on the vessel, dates, locality, depth, collecting gear, collection effort, and total number of specimens

Cruise	Vessel	Date	Locality	Depth	No. of specimens (collection effort)
C3 ^a	OSV Maersk Launcher	3 April–6 June 2018	NORI-D	4115 m	One specimen (from box core)
C5A	OSV Maersk Launcher	16 October–30 November 2020	NORI-D	4121–4320 m	Four specimens (3/4896 specimens processed from 53 box cores; one from multicore)
C6B ^a	OSV Maersk Launcher	10 November–22 December 2019	NORI-D	4173–4294 m	Three specimens (81 box cores)
JC241	RRS James Cook	4 February–26 March 2023	Site of the Ocean Minerals Company (OMCO) track (Jones <i>et al.</i> 2025)	4700 m	One specimen (783 samples processed from 40 box cores)

^aSamples from these cruises were acquired months after collection and none of the authors nor their teams were involved in the planning of the cruises nor joined the expeditions.

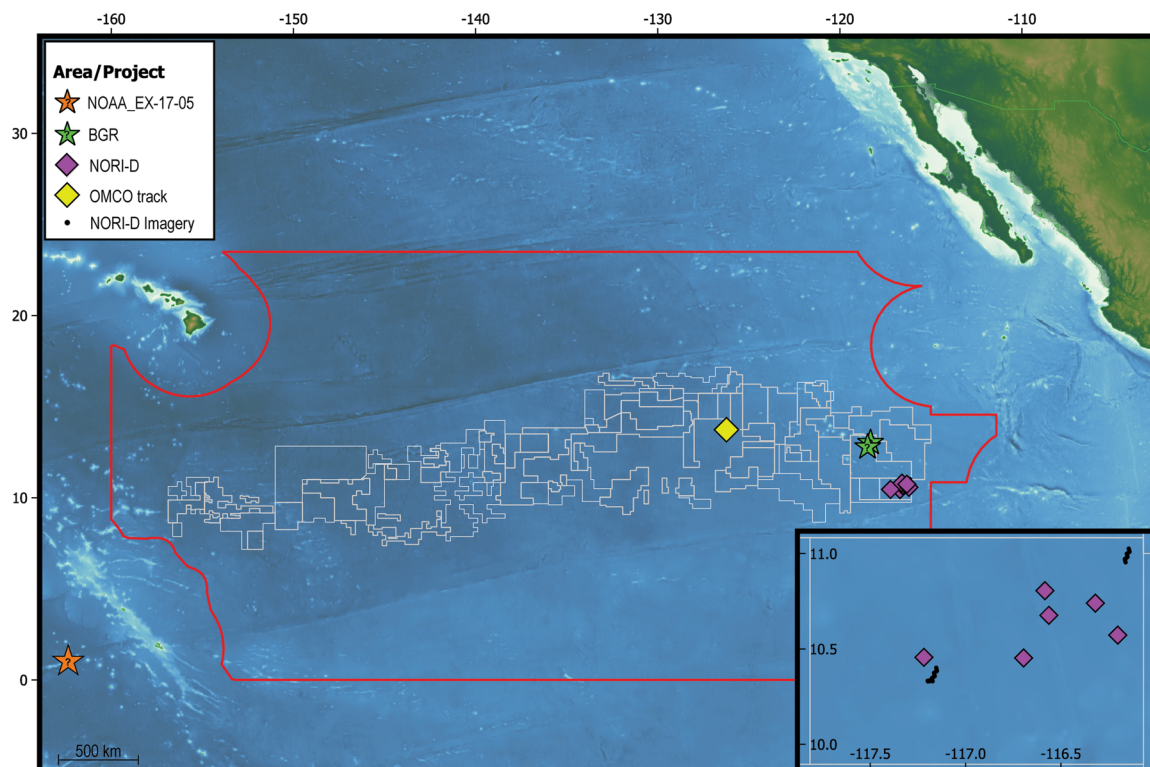


Figure 1. Map of the Clarion-Clipperton Zone (red outline) indicating samples collected in NORI-D (purple \diamond) and in the site of a trial mining operation conducted by the Ocean Minerals Company (OMCO) in 1979 (yellow \diamond); records from the NORI-D seabed imagery survey carried out in 2021 (black dots). Additional suspected records obtained from imagery available at OBIS public databases (Hourigan 2020) and from Uhlenkott *et al.* (2022) are shown in orange (\star) and green (\star), respectively. Exploration and reserved areas are outlined in white. Insert of the NORI-D exploration area indicating samples collected (purple \diamond) and samples observed from seabed imagery transects (black dots).

damaged the calcium carbonate skeleton and completely dissolved one of the smallest specimens. DNA extraction using QuickExtract was less damaging, allowing the recovery of the corallite of another small specimen.

The PCR mix for each reaction contained 10.5 μ l of Red Taq DNA Polymerase 1.1 \times MasterMix (VWR), 0.5 μ l of each primer (10 μ M), and 1 μ l of DNA template. The mitochondrial gene cytochrome oxidase subunit I (COI) was amplified using the primers LCO1490 (GGTCAACAAATCATAAAGATATTGG) and

HCO2198 (TAAACTTCAGGGTGACCAAAAAATCA) (Folmer *et al.* 1994) with an initial denaturation at 95°C for 5 min, followed by 35 cycles of denaturation at 95°C for 45 s, annealing at 49°C for 45 s, and extension at 72°C for 1 min, with a final extension of 72°C for 10 min. The long ribosomal gene (28S) was amplified using the primers 28S-Far (5'-CACGAGACCGATAGCGAA CAAGTA-3') and 28S-Rar (5'-TCATTTCGACCC TAAGACCTC-3') (McFadden and van Ofwegen 2012) with an initial denaturation at 94°C for 3 min, followed by 35 cycles of

denaturation at 94°C for 30s, annealing at 50°C for 30s, and extension at 72°C for 1 min, with a final extension at 72°C for 5 min. Amplicons were purified and sequenced at the NHMUK Sequencing Facilities using a Millipore Multiscreen 96-well PCR Purification System and an ABI 3730XL DNA Analyser (Applied Biosystems), respectively. Contigs were *de novo* assembled using Geneious 7.0.6 (<https://www.geneious.com>) with default settings and trimming the primer sequences. Ambiguous base calls were corrected manually, and translated to amino acids (*COI* only) to look for stop codons, and compared against public databases to remove unwanted sequences. DNA sequences generated in this study were submitted to GenBank (*COI*: PV826147–PV826149; 28S: PV822267–PV822271). DNA extractions have been deposited at the Molecular Collections Facility (MCF) at the NHMUK.

Phylogenetic inference and genetic divergence

Phylogenetic inference was performed to investigate the phylogenetic placement of the new species collected in the CCZ. The sequences for the 28S and *COI* genes used in Kitahara *et al.* (2013) were downloaded from NCBI and used for phylogenetic inference. Sequences from both *COI* and 28S were aligned using MAFFT v.7, using the FFT-NS-I strategy (Katoh *et al.* 2019). Phylogenetic inference on each locus was performed separately using a maximum likelihood and a Bayesian inference approach. Maximum likelihood analyses were conducted in RAxML (Stamatakis 2006) using the best substitution models (*COI*: GTR+G with codon partitions 1,2,3; 28S: GTR+G) as estimated in PartitionFinder2 (Lanfear *et al.* 2017), with rapid Bootstrap, and node support estimated from 1000 bootstrap replicates. Bayesian inference analyses were conducted in MrBayes (Huelsenbeck and Ronquist 2001) using the best substitution model (*COI*: GTR+I+G for codon partitions 1,3, and HKY+I for codon partition 2; 28S: GTR+I+G), two Markov chain Monte Carlo (MCMC) chains of 1 million generations each and 25% burn-in. Effective Sample Sizes (ESS) were checked (> 100) and sampled trees were summarized.

Corrected intraspecific and interspecific genetic divergence (K2P; Kimura 1980) were estimated for both alignments in Mega-X (Kumar *et al.* 2018). Variance was estimated through 100 bootstraps. Intraspecific genetic distances were only estimated for the new species because there is a single sequence available for each of the other species included in the analyses.

RESULTS

Taxonomy

Order Scleractinia

Suborder Vacatina Okubo, 2016 ('Robust' clade)

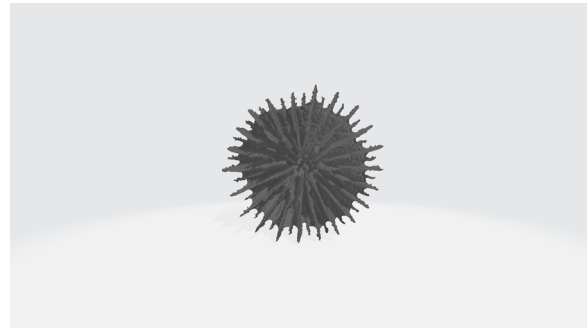
Family Deltocyathidae Kitahara, Cairns, Stolarski & Miller, 2013

Genus *Deltocyathus* Milne Edwards & Haime, 1848

Deltocyathus zoemetallicus Santodomingo, Bribiesca-Contreras & Kitahara **sp. nov.**

(Figs 2–3, Model 1)

ZooBank registration: urn:lsid:zoobank.org:act:9D13E49F-F882-424A-898C-1BFAE63851CE.



Model 1. *Deltocyathus zoemetallicus* 3D model of holotype (specimen number NHMUK 2025.1) from micro-computed tomography (μ CT).

Type locality: NORI-D, Clarion Clipperton Zone, Pacific Ocean, 4278 m depth (OSV Maersk Launcher BC_339 station STM_003, 10.3226, -117.1873).

Type material: **Holotype:** NHMUK 2025.1 - Adult (GCD = 7.9 mm) attached to nodule, preserved in 80% EtOH; NORI-D, Clarion-Clipperton Zone, Pacific Ocean; Cruise C5A, deployment BC_339, station STM_003 (05/11/2020, 10.3226/-117.1873, 4278 m depth), collected by Helena Wiklund (H.W.), Guadalupe Bribiesca-Contreras (G.B.C.), Regan Drennan (R.D.), Corie Boolukos (C.B.), Thomas G. Dahlgren (T.G.D.), Adrian G. Glover (A.G.G.); GenBank: PV822267 (28S), PV826147 (*COI*); NHMUK MCF FD16415932; field code: NHM_5312.

Paratypes: NHMUK 2025.2 - Adult (GCD = 4.5 mm) attached to nodule, preserved in 80% EtOH; NORI-D, Clarion-Clipperton Zone, Pacific Ocean; Cruise C5A, deployment BC_353, station SWM_023 (10/11/2020, 10.4753/-117.385, 4291 m depth), collected by H.W., G.B.C., R.D., C.B., T.G.D., A.G.G.; GenBank: PV822268 (28S); NHMUK MCF FD16412816; field code: NHM_5788. **NHMUK 2025.4** - Adult (GCD = 7.5 mm) attached to nodule, preserved in 80% EtOH; NORI-D, Clarion-Clipperton Zone, Pacific Ocean; Cruise C3, deployment BC_031, station BC_031 (43243, 10.4522/-116.6956, 4115 m depth), collected by H.W., G.B.C., R.D., C.B., T.G.D., A.G.G.; field code: NHM_8925. **NHMUK 2025.5** - Juvenile (GCD = 1.1 mm) attached to nodule, preserved in 80% EtOH; OMCO track, Clarion-Clipperton Zone, Pacific Ocean; Cruise JC241, deployment JC241_061, station OMCO Track (44986, 13.7359/-126.2204, 4712 m depth), collected by G.B.C., Belen Arias (B.A.), Lucas King (L.K.), Eva Stewart (E.S.), Daniel O.B. Jones (D.O.B.J.), A.G.G.; GenBank: PV822269 (28S), PV826148 (*COI*); NHMUK MCF FD16413042; field code: NHM_10983. **NHMUK 2025.6** - Adult (GCD = 6.6 mm) attached to nodule, preserved in 80% EtOH; NORI-D, Clarion-Clipperton Zone, Pacific Ocean; Cruise C6B, deployment BC_199, station X (43798, 10.6763/-116.5629, 4173 m depth), collected by H.W., G.B.C., R.D., C.B., T.G.D., A.G.G.; field code: ND6B1234. **NHMUK 2025.7** - Adult (GCD = 5.8 mm) attached to nodule, preserved in 80% EtOH; NORI-D, Clarion-Clipperton Zone, Pacific Ocean; Cruise C6B, deployment BC_204, station AC (43799, 10.8056/-116.584, 4294 m depth), collected by H.W., G.B.C., R.D., C.B., T.G.D., A.G.G.; field code: ND6B1501. **NHMUK 2025.8** - Adult (GCD = 7.9 mm) attached to nodule, preserved in 80% EtOH; NORI-D, Clarion-Clipperton Zone,

Pacific Ocean; Cruise C6B, deployment BC_209, station AH (43799, 10.5722/-116.2018, 4174 m depth), collected by H.W., G.B.C., R.D., C.B., T.G.D., A.G.G.; field code: ND6B1748. **NHMUK 2025.9** - Adult (GCD = 7 mm) attached to nodule, preserved in 80% EtOH; NORI-D, Clarion-Clipperton Zone, Pacific Ocean; Cruise C6B, deployment BC_214, station AM (43806, 10.4559/-117.2186, 4271 m depth), collected by H.W., G.B.C., R.D., C.B., T.G.D., A.G.G.; field code: ND6B3533. **NHMUK 2025.10** - Adult (GCD = 7.9 mm) attached to nodule, preserved in 80% EtOH; NORI-D, Clarion-Clipperton Zone, Pacific Ocean; Cruise C6B, deployment BC_245, station AAAAD (43801, 10.7404/-116.3192, 4193 m depth), collected by H.W., G.B.C., R.D., C.B., T.G.D., A.G.G.; field code: ND6B1997.

Additional material: **NHMUK 2025.3** - Adult, broken (GCD=0 mm) attached to nodule, preserved in 80% EtOH; NORI-D, Clarion-Clipperton Zone, Pacific Ocean; Cruise C5A, deployment MC_065, station STM_016 (19/11/2020, 10.4285/-117.1484, 4320 m depth), collected by H.W., G.B.C., R.D., C.B., T.G.D., A.G.G.; GenBank: PV822270 (28S); NHMUK MCF FD16415437; field code: NHM_6383. **Juvenile** (GCD = 1.3 mm; specimen lost) attached to nodule; NORI-D, Clarion-Clipperton Zone, Pacific Ocean; Cruise C5A, deployment BC_375, station SPR_042 (21/11/2020, 10.844/-116.2455, 4121 m depth), collected by H.W., G.B.C., R.D., C.B., T.G.D., A.G.G.; GenBank: PV822271 (28S), PV826149 (COI); NHMUK MCF FD16413049; field code: NHM_6484.

Diagnosis: *Deltocyathus* attached to polymetallic nodules, with septa arranged in four cycles. All septa, except for S4, bear a prominent paliform lobe (P1–P3) that rise as high or higher than its respective septum, especially in juvenile specimens.

Description: Corallum trochoid to turbinate, straight to slightly curved, distally flared (Fig. 2A, E, H, K), and firmly attached to a polymetallic nodule by a robust pedicel (Fig. 2A); base monocyclic (Supporting Information, Fig. S1). Pedicel base slightly concave to conform with the rounded nodule surface. Juvenile specimens short and turbinate (Fig. 3C, F). Calice circular with an evenly serrated calicular margin (Fig. 2B–D, F–G, I–J). Holotype 7.9 mm in CD, 5.2 mm in H, and 3.4 mm in PD is the largest specimen examined, but one imaged specimen (not sampled) attained 12.1 mm in CD. Costae ridged and coarsely granular. Costal granules sharp and irregular. C1–4 about same width. Costae extend from the calicular edge to the base, but some C3–4 extend only halfway. Intercostal furrows about half the width of costae near base but progressively widening towards calicular margin, where they are up to twice as wide than costae. Corallum uniformly white. A thin translucent tissue encapsulates most of the corallum, disappearing around the pedicel.

Septa hexamerally arranged in four complete cycles according to the formula: $S1 > S2 > S3 > S4$. Holotype with incomplete S4 (44 septa; Fig. 2A–F), though paratypes NHMUK 2025.8 (Fig. 2G–I) and NHMUK 2025.10 (Fig. 2J–L) have all septal cycles complete (48 septa). S1 highly exsert (up to 0.7 mm exsert), projects slightly outside from calicular margin, independent, extends two-thirds the distance to the columella, and bears one large paliform lobe. S2 slightly smaller but otherwise similar to S1. S3

three-quarters of the width of S2, and bears a paliform lobe that joins P2 near the columella. S4 small and sometimes reduce to a row of spines, though joins S3 at the septal base deep in the fossa. S1–3 septal faces bear low vertically aligned granules. Septal axial margins slightly sinuous, or even forming a short carinae. Paliform lobes rise as high or slightly higher than septa, from which they are separated by a deep and wide notch. Three palar crowns easily distinguishable ($P1 > P2 > P3$) and progressively more recessed from the columella. Fossa deep containing a papillose columella formed by 6–8 interconnected papillae.

Morphological remarks: Among the 26 valid species in the genus *Deltocyathus* (Hoeksema & Cairns, 2025), only *Deltocyathus halianthus* (Lindström, 1877) and *D. zoemetallicus* were attached in their adult phase. Endemic from shallow waters of Brazil (46–180 m depth), *D. halianthus* differed from *D. zoemetallicus* in having a tympanoid corallum, a polycyclic base (up to five cycles), septa with serrate margins, and costae with sparse, hollow warts, or spines. Although there was no molecular data for *D. halianthus*, it has been suggested that such morphological characters have some affinity with members of Rhizangiidae (Cairns 2000). In contrast, molecular phylogenetics (Fig. 5) showed that *D. zoemetallicus* was part of the *Deltocyathus* clade, as a sister species of the free-living *Deltocyathus heteroclitus* Wells, 1984. The latter is known from the Late Pleistocene (type locality Espiritu Santo, Vanuatu) to the Present (Wallis and Futuna, Vanuatu, and New Caledonia, 80–1270 m depth). *Deltocyathus heteroclitus* can be distinguished from *D. zoemetallicus* and other congeners by its polygonal corallum, slightly conical base, and eight costal spines (C3) (Kitahara and Cairns 2021). Among other *Deltocyathus* species with four septal cycles that lack costal spines, and have a white corallum, *D. zoemetallicus* most resembles the free-living Indo-Pacific congeners *D. murrayi* and *D. crassiseptum*, and the Atlantic species *Deltocyathus moseleyi* (Cairns, 1979). From them, the bowl shape of the corallum of *D. crassiseptum*, in addition to its flat base and thicker septa with conspicuous septal granules differentiates it from *D. zoemetallicus*. Perhaps the closest morphological species to *D. zoemetallicus* is *D. murrayi*, as both have thin septa and fewer columella elements (< 10 interconnected papillae). However, *D. murrayi* differs in having a conical/diamond-shaped corallum, a larger S4 following the septal formula: $S1 > S2 \geq S4 > S3$ or $S1 > S4 \geq S2 > S3$, and by having a larger adult size with CD 16–22 mm (Kitahara and Cairns 2021), which is two to three times the corallum size of *D. zoemetallicus*. The bowl shape, septa arrangement, and rounded base of the Atlantic species *D. moseleyi* (Cairns 1979) also contrasts with the cup and attached form of *D. zoemetallicus*.

Etymology: The species name *zoemetallicus* from the Greek words ζωή (zoí) meaning ‘life’ and μεταλλικός (metallikós) meaning ‘relating to metal’ refers to the species living attached to polymetallic nodules. It is also named after the first author’s daughter, Zoë Judy Bribiesca-Miller.

Distribution and ecology: *Deltocyathus zoemetallicus* occurs in the eastern central Pacific, in the CCZ, from 4115 to 4712 m depth. The species is found attached to polymetallic nodules and has not yet been collected as free-living or attached to other types of substrates in the area.

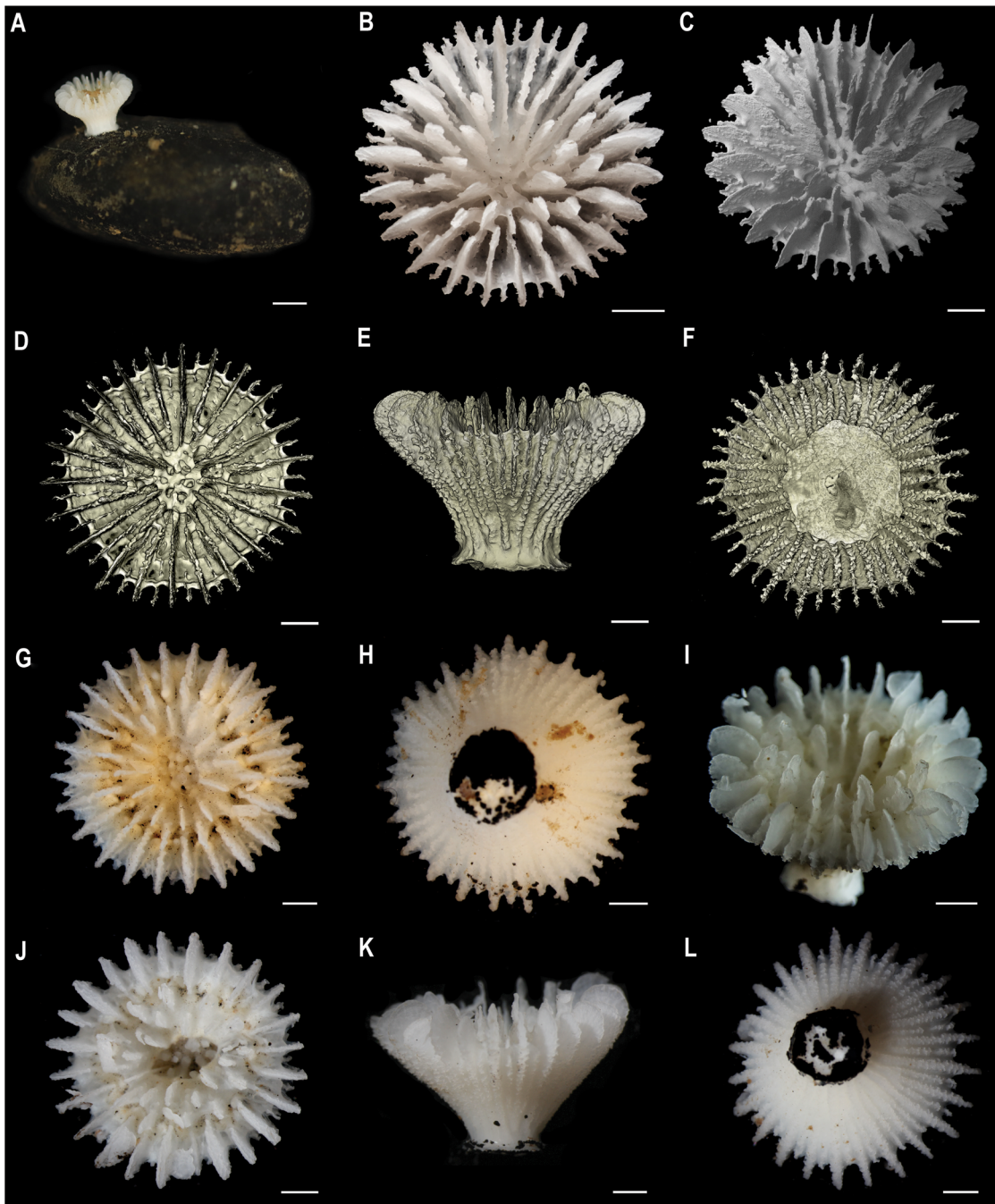


Figure 2. *Deltocyathus zoemetallicus*. Holotype, specimen number NHMUK 2025.1: (A) specimen still attached to a polymetallic nodule; (B) calicular view of a clean corallum; (C) calicular view of SEM; (D) calicular view of μ CT scan; (E) scan lateral view from μ CT scan; (F) basal view from μ CT scan. Paratype, specimen number NHMUK 2025.8: (G) calicular view; (H) basal view. Paratype, specimen number NHMUK 2025.9: (I) lateral view. Paratype, specimen number NHMUK 2025.10: (J) calicular view; (K) lateral view; (L) basal view. Scale bars: A, 5 mm; B–L, 1 mm.

Despite relatively extensive sampling in the region, the species has been quite rarely recovered. Specimens of *D. zoemetallicus* have only been collected from the NORI-D exploration area and at a second site located 1000 km to the northwest, at the site of a trial mining operation conducted by the Ocean Minerals Company (OMCO) in 1979 (Jones *et al.* 2025). In addition, a morphotype (*Deltocyathidae* gen. indet. mtp-SCL_002) assigned to the family *Deltocyathidae* has been reported from seabed imagery

in the Federal Institute for Geosciences and Natural Resources of the Federal Republic of Germany (BGR) exploration contract area (Uhlenkott *et al.* 2023), a few kilometres north of NORI-D (Fig. 1, green star). These latter specimens were only observed attached to very large pillow lava rock outcrops, with none observed on nodules. Based on the closeness of the BGR site to the main collecting site, and on figure 6d from Uhlenkott *et al.* (2023) where the shape of the corallum is clearly visible,

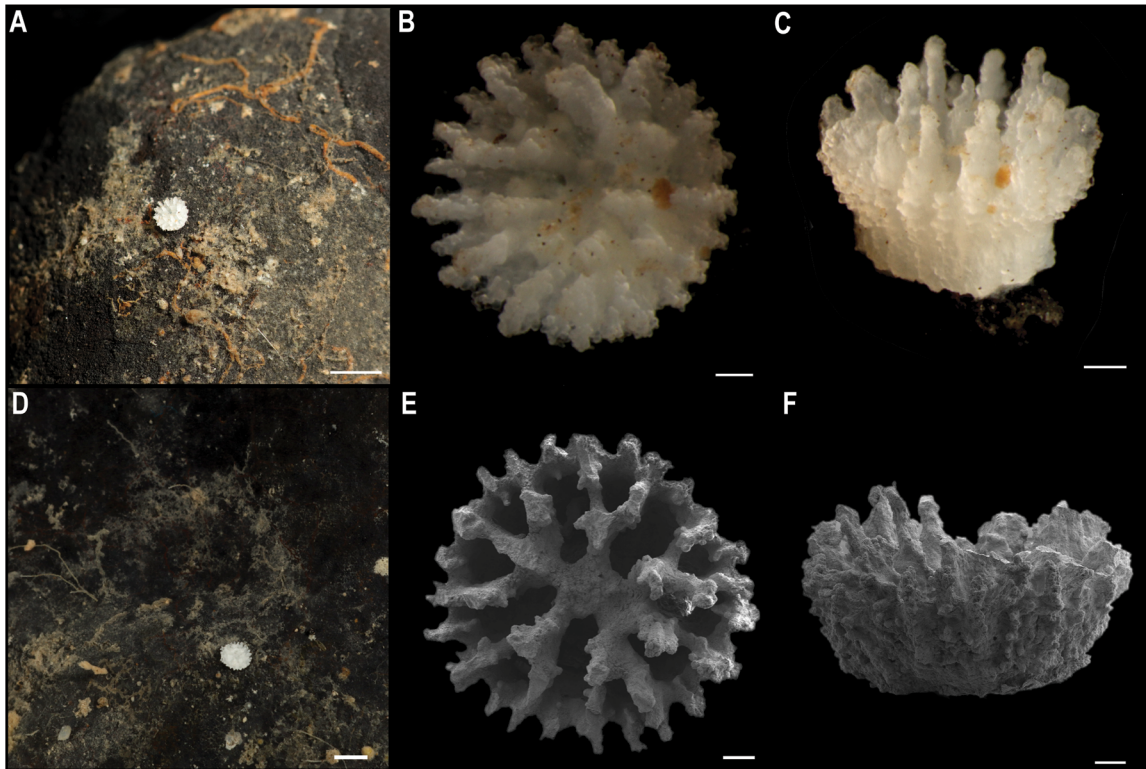


Figure 3. *Deltocyathus zoemetallicus*. Juvenile (MCF FD16413049): (A) attached to nodule; (B) calicular view; (C) lateral view. Paratype, juvenile, specimen number NHMUK 2025.5: (D) attached to nodule; (E) SEM calicular view; (F) SEM lateral view. Scale bars: A, 2 mm; B–C, 200 μ m; D, 1 mm; E–F, 100 μ m.

including prominent paliform lobes, it is very likely that these specimens should be assigned to *D. zoemetallicus*, which would further extend the range of the species in geographic range and ability to live on substrates other than nodules. Two additional records, likely belonging to this species (Fig. 1, orange star), were found on the Ocean Biodiversity Information System (OBIS 2025). They are located about 5000 km west off the CCZ and within the depth range (4368–4390 m) of the species (occurrenceID: NOAA_DSCRTP: 927805, NOAA_DSCRTP: 927808; Hourigan 2020).

Density estimates

Density (individuals per ha) was estimated for NORI-D from a seabed imagery survey carried out in 2021 (Fig. 4). A total of 835 individuals were observed in 12668 images from three areas within NORI-D: the Collector Test Area (CTA), the Mining Area (MIN), and the Preservation Reference Zone (PRZ; Fig. 4B–D). The images covered a total area of 7776 m² (CTA = 1855 m², MIN = 1702 m², and PRZ = 4219 m²). The calicular diameter of the annotated specimens ranged from 1.47 to 12.1 mm (mean = 5.25 mm, median = 5.15). After excluding all specimens with CD < 2.5 mm, 795 individuals were retained for analyses (CTA = 280 individuals, MIN = 269 individuals, and PRZ = 246 individuals). The average density of the new species of cup coral was 1222 ± 312 ind/ha, being similar in the CTA and MIN areas (1519 ± 256 ind/ha and 1598 ± 427 ind/ha, respectively), and significantly lower in the PRZ [548 ± 384 ind/ha; $F_{(2,12)} = 20.00$, $p < .001$; $\text{Eta}^2 = 0.77$, 95% CI (0.50, 1.00); Fig. 4A].

Phylogenetic analyses of the COI and 28S genes

Phylogenies estimated from both maximum likelihood and Bayesian inference for both COI and 28S loci recovered all species of *Deltocyathus* in a well-supported monophyletic clade, although the relationships between species within the genus were not resolved. The specimens of the new species were not recovered in a monophyletic clade in the COI phylogeny (Fig. 5A), but they were recovered with high support in the 28S phylogeny (Fig. 5B). In both phylogenies, *D. heteroclitus* was recovered close to the new species, albeit with very low support (< 0.7 or 70) for 28S.

Intraspecific divergence was 0 to 0.35% for COI, and 0% for 28S (Table 2). Interspecific divergence varied from 0 to 2.31% for COI, and 0 to 2.8% for 28S. The COI sequence of *D. heteroclitus* was identical to the sequence from two specimens of the new species. However, the 28S sequence of *D. heteroclitus* varied between 0.62 and 1.7% from sequences of *D. zoemetallicus*.

DISCUSSION

Deltocyathus zoemetallicus represents the first azooxanthellate scleractinian coral to be found attached to polymetallic nodules. Also, it is only the second species in the genus *Deltocyathus* to be found attached in the adult stage, while all the other congeners are known to be free-living as adults (Kitahara *et al.* 2013), even if they attach to hard substrates in earlier life stages (e.g. *Deltocyathus corrugatus* Cairns, 1999). Late attachment of free-living scleractinians has also been reported in other coral taxa, such as *Fungia fungites* (Linnaeus, 1758), in which juvenile buds usually detach

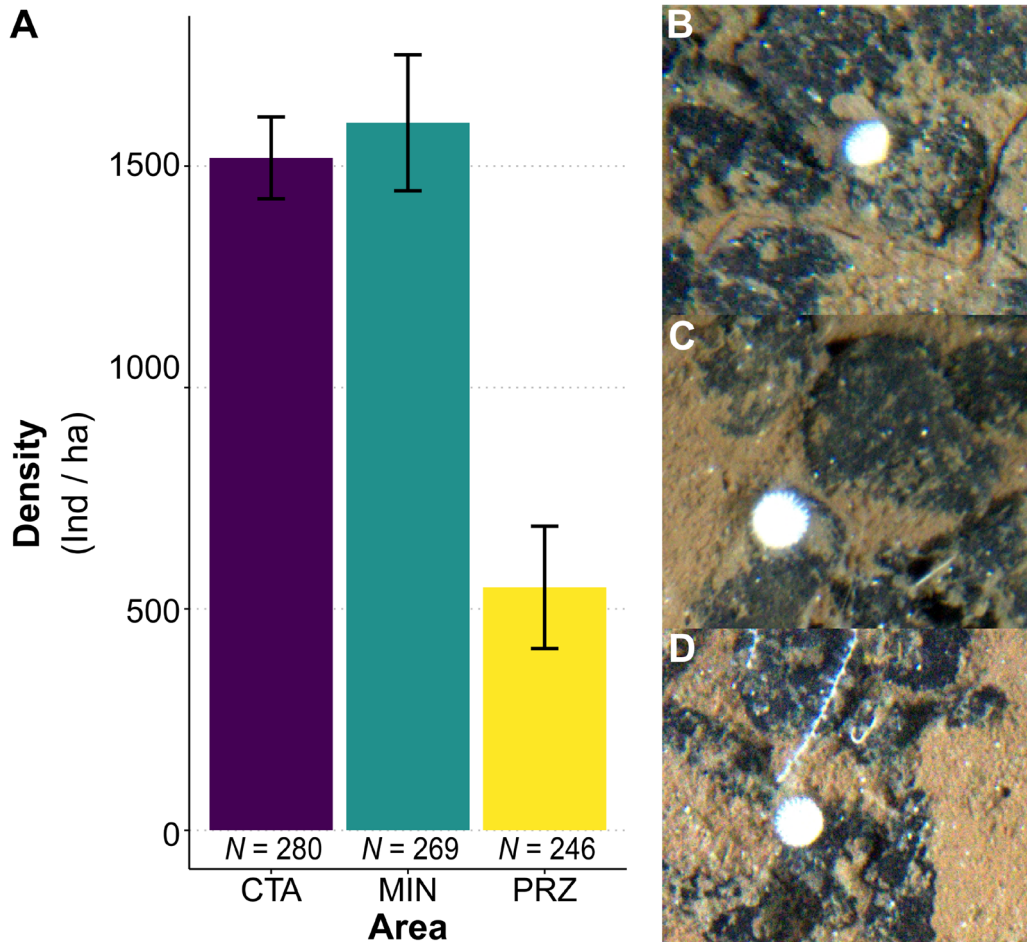


Figure 4. A, barplot indicating densities (ind/ha) of *Deltocyathus zoemetallicus* estimated from seabed imagery from three transects carried out in the NORI-D area in 2021. Total number of specimens counted in each transect is indicated below the bar (*N*). B–D, examples of seabed images. CTA, Collector Test Area; MIN, Mining Area; PRZ, Preservation Reference Zone.

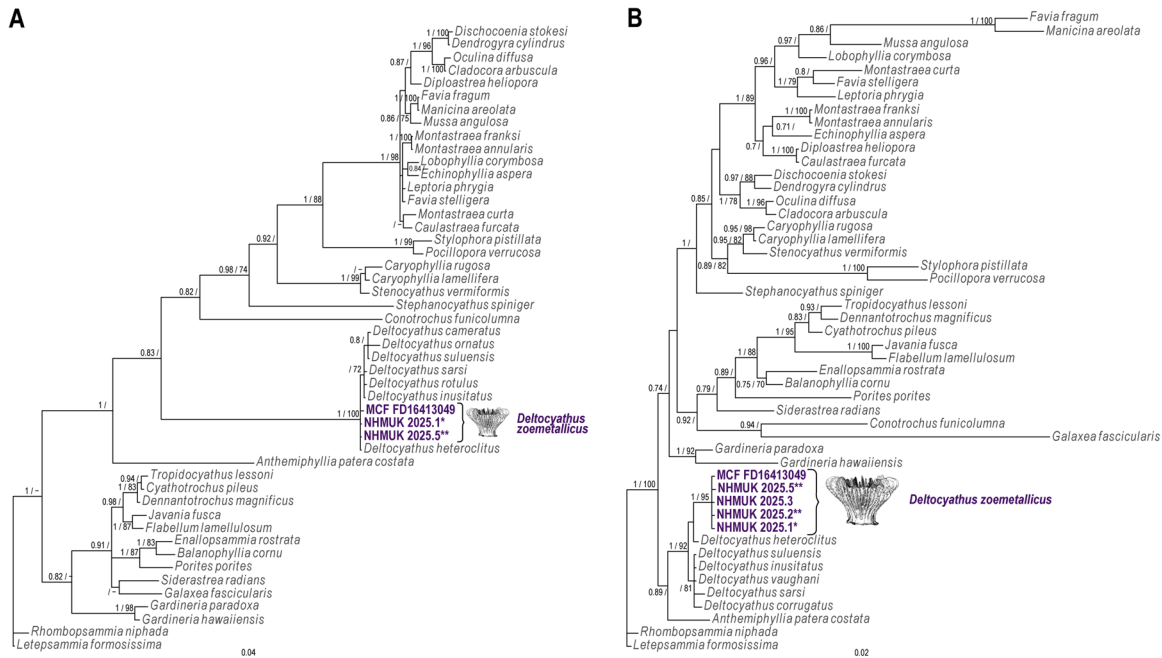


Figure 5. Bayesian phylogenetic trees for Scleractinia estimated from COI (A) and 28S (B). Median consensus trees showing posterior probability and bootstrap support values at each node (PP/BS). Only values higher or equal to 0.7 or 70 for PP or BS are indicated. ‘?’ indicates the node was not recovered in the Maximum Likelihood phylogeny. * Holotype; ** Paratypes.

Table 2. Corrected (K2P) genetic distances for members of the genus *Deltocyathus* given as a percentage (%). Interspecific genetic distances for 28S are shown below the diagonal, and above the diagonal for COI. Intraspecific genetic distances only shown for the new species

	<i>D. corrugatus</i>	<i>D. sarsi</i>	<i>D. vaughani</i>	<i>D. inusitatus</i>	<i>D. suluensis</i>	<i>D. heteroclitus</i>	<i>D. rotulus</i>	<i>D. ornatus</i>	<i>D. cameratus</i>	<i>D. zoemetallicus</i>
<i>D. corrugatus</i>										
<i>D. sarsi</i>	0.81	^a								
<i>D. vaughani</i>	0.32	0.49		0.17						
<i>D. inusitatus</i>	0.32	0.49	0.00		0.34					
<i>D. suluensis</i>	0.32	0.49	0.00	0.00		0.34				
<i>D. heteroclitus</i>	0.65	0.81	0.32	0.32	0.32		0.51			
<i>D. rotulus</i>	–	–	–	–	–	–		1.70		
<i>D. ornatus</i>	–	–	–	–	–	–	0.34		0.68	
<i>D. cameratus</i>	–	–	–	–	–	–	–	1.53		
<i>D. zoemetallicus</i>	0.95–2.00	1.91–2.88	0.95–2.00	0.95–2.00	0.95–2.00	0.63–1.71	–	1.19	0.51	
							0.51	1.88	0.17	0.51–0.88
							0.51	1.36	0.85	0.33–0.70
							–	0.68	0.68	0.68–1.06
							–	–	1.36	0.00–0.35
							–	–	–	0.37–0.88
							–	–	–	1.88–2.31
							–	–	–	0.85–1.23
							–	–	–	0.00–0.35
							–	–	–	0.0

^aNot estimated as there were no sequences available.

before reaching 5 cm, although larger attached specimens have also been reported (Hoeksema and Yeemin 2011). The specimens collected from *D. zoemetallicus* range from 1.1 to 7.9 mm CD, with the two smallest displaying juvenile characteristics. These juvenile specimens possess the diagnostic features of adults but have only three complete septal cycles (24 septa), instead of four, and a short, turbinate corallum. Larger specimens, > 4.5 mm in CD, have four cycles and a consistent corallum shape with a well-developed pedicel. This indicates that both juvenile and adult life stages of *D. zoemetallicus* attach to hard substrate, but the pedicel develops at a later growth stage. Moreover, all 795 individuals recorded in the ROV survey were observed on nodules, including the largest specimens (>12.1 mm in CD). The dual life-mode that includes attached and free-living congeneric species has also been described for other coral genera originally thought to be exclusively free-living, such as mushroom corals in the genus *Cycloseris* Milne Edwards & Haime, 1848, with 12 free-living species and two attached species (Benzoni *et al.* 2012).

Phylogenetic trees for both *COI* and 28S supported the placement of the new species within the genus *Deltocyathus*. However, the relationships between the different species were not resolved in either of the phylogenies. Despite *COI* being used widely for species barcoding (Hebert *et al.* 2003), the slow evolution of the *COI* gene in anthozoans prevents its use as a reliable barcoding system (Huang *et al.* 2008, Shearer and Coffroth 2008). An overlap between intra- and interspecific genetic distances for *COI* was observed with an interspecific genetic distance of 0 to 2.31% and intraspecific genetic distance of 0 to 0.35%. The *COI* sequences of two specimens from the new species are identical to the sequence of *D. heteroclitus*. However, this is not uncommon among scleractinian corals. One comprehensive study of 90 reef-coral species, representing 44 genera in 14 families of taxa worldwide, found that 40% of congeners showed 0% divergence in *COI* sequences, yet all species had different morphological characteristics (Shearer and Coffroth 2008).

Deltocyathus zoemetallicus and *D. heteroclitus* are also very distinct morphologically. They differ in the overall shape of the corallum, while *D. heteroclitus* has a polygonal calicular outline and up to eight blunt spines projecting horizontally (Wells 1984), the calicular outline of the new species is rounded with no spines. Scleractinian corals can exhibit high morphological plasticity in skeletal structures as a result of environmental conditions (Todd 2008). Hence, it has been suggested that additional information on their ecology, life-history traits, and behaviour needs to be considered for defining species boundaries (Maté 2003). These two species also differ in *D. heteroclitus* being free-living in soft sediments while *D. zoemetallicus* attaches to hard substrates. They are also found at different depth ranges. *Deltocyathus heteroclitus* has been reported from 80 to 1270 m deep, with all records in the west Pacific. The new species has a much deeper distributional range, from 4115 to 4712 m, and is distributed in the CCZ (eastern Pacific), possibly spanning the entire CCZ and adjacent areas where hard substrates are available in the form of polymetallic nodules, crusts, or rock outcrops. Compared to the other attached Atlantic species, *D. halianthus*, they both share a similar rounded corallite outline, lack of projecting spines, and the same septal arrangement (Cairns 2000). Yet, they differ in that *D. zoemetallicus* has diagnostic high paliform lobes, fewer columella elements, and

a monocyclic base. In addition, *D. halianthus* is a shallow-water species (46–130 m depth) found only in the coast of Brazil, attached to bivalve shells (Cairns 2000, Kitahara 2007).

All collected *D. zoemetallicus* specimens were attached to nodules, as well as the specimens observed from seabed imagery in NORI-D. Sample collection in the CCZ is almost exclusively done using corers in soft-sediment habitats, including video surveys. This sampling bias prevents drawing any conclusions about the distribution of the new species on adjacent rock outcrops. Interestingly, the suspected additional records—based on seabed images only—coming from west of the CCZ (Hourigan 2020) and from the BGR contractor exploration area (Uhlenkott *et al.* 2023) were observed attached to rock outcrops. In the latter study, it was suggested that the observed cup coral, which we suspect could be assigned to *D. zoemetallicus* based on the diagnostic morphological traits visible in the images, is a specialist of rock outcrops and was not found on nodules. Previous megafaunal studies in the CCZ excluded any fauna smaller than 10 mm (e.g. Amon *et al.* 2016, Simon-Lledó *et al.* 2019a, b), including the study by Uhlenkott *et al.* (2023). However, none of the specimens collected in our study reached that diameter threshold, the largest specimen being 7.9 mm, and only six individuals from the imagery data (representing 0.007%) potentially reach about 10 mm (Supporting Information, Fig. S2). If cup corals that settle on rock outcrops can grow to larger sizes than those on nodules, as suggested by the reported correlation between patch size and animal size (Mejía-Saenz *et al.* 2023), then the smaller specimens attached to nodules would have been excluded from all previous megafaunal studies.

The small size of the adult of this species excludes them from most seabed imagery analyses. However, images taken closer to the seabed than usual during a 2021 survey allowed the identification of *D. zoemetallicus*, enabling the estimation of its abundance on polymetallic nodules in the NORI-D exploration area. Standing stocks were estimated to be an order of magnitude higher than some octocorals in nodule areas of the CCZ (Mejía-Saenz *et al.* 2023). Within NORI-D, standing stocks were significantly lower in the PRZ (548 ± 384 ind/ha) compared to the CTA (1519 ± 256 ind/ha) and MIN (1598 ± 427 ind/ha) areas. The CTA and MIN areas are characterized by a high density of small nodules that almost completely cover the seafloor, whereas the PRZ nodule coverage varies from areas densely covered with small nodules to sectors with larger but sparse nodules, or even areas with no nodules (Fleming *et al.* 2025). This suggests that standing stocks of *D. zoemetallicus* might depend on the nodule density, thus making the species locally vulnerable to potential deep-sea mining activities even if their broader range extent confers them with some resilience at larger scales.

Despite several expeditions to the CCZ, including at least 12 cruises and over 400 box core deployments in which our teams have been involved in or had access to samples, only 11 specimens of *D. zoemetallicus* have ever been collected, with all but one from the NORI-D exploration area. While the high collection effort yielding only a few specimens might suggest that this species is rare, as is typical for most deep-sea species (McClain 2021), it could also reflect under-sampling. The CCZ spans over 6 million km² and is characterized by high habitat heterogeneity (Wedding *et al.* 2013, Kaiser *et al.* 2017). In this vast area, 400 box cores represent a minimum sampled fraction of just over 0.0001 km².

Conversely, this level of sampling has provided insights into the distribution and connectivity of other small sessile species that are relatively common, such as the demosponge *Plenaster craigi* Lim & Wiklund, 2017, with a maximum body size that varies from 3.6 to 17.8 mm. This encrusting sponge is widely distributed across the eastern CCZ occurring from 4041 to 4183 m and spanning over 800 km (Lim *et al.* 2017), and exhibits a strong geographic genetic structure beyond what would be expected by distance alone (Taboada *et al.* 2018). The absence of this demosponge in deeper sites more centrally located in the CCZ at more than 4680 m in depth (Jones *et al.* 2025), is in accordance to recent findings of demosponges being restricted to areas above the carbonate compensation depth (CCD) (Simon-Lledó *et al.* 2023b). In contrast, specimens of *D. zoemetallicus* have not been observed as commonly as *P. craigi* but they occur deeper, with a specimen collected at the OMCO site at 4712 m. The presence of a thin, translucent tissue that encapsulates most of the corallum possibly allows this species to live below the CCD. Additional sampling covering larger areas and additional genetic markers would be needed to understand the distributional and connectivity patterns of the new species.

The results of this study suggest that the new species *D. zoemetallicus* likely occurs across multiple habitat types, has a wider bathymetric range likely not restricted by the CCD, and a geographic range beyond 1000 km. Despite this broad geographic range that may confer resilience at a large scale, the new coral species could be locally vulnerable to potential deep-sea mining activities. Further studies should focus on species distribution assessments, connectivity, and the contribution of rocky areas to local biodiversity in the CCZ. Rocky areas may serve as a potential refuge for some nodule-attached species and could act as stepping stones to facilitate population connectivity.

ACKNOWLEDGEMENTS

We thank the captain and crew of the OSV Maersk Launcher, and of the RRS James Cook, as well as the teams on board that assisted with data collection and sample processing, especially to our NHMUK colleagues Regan Drennan, Corie Boolukos, Belen Arias, Lucas King, and Eva Stewart. We are also grateful to Claire Dalglish and Toby Adamson for managing at-sea operations during the cruise CSA, and Leigh Marsh for providing access to additional samples from the NORI-D environmental programme. We thank NHMUK curatorial staff Miranda Lowe, Tom White, Lauren Hughes, and Heather Avrili for their support. We are grateful to NHMUK staff for their technical expertise: Claire Griffin for assistance with sequencing, Alex Ball and Innes Clatworthy for support using the SEM, Brett Clark for generating the μ CT scan, and Georgina Glasier for support with logistics. This publication is contribution TMC/NORI/D/028.

AUTHOR CONTRIBUTIONS

G.B.C. and N.S. conceived the study. T.G.D., D.O.B.J., and A.G.G. contributed the specimens and generated the images. G.B.C., N.S., M.V.K., E.S.-L., and B.F.M.F. generated and analysed the data. G.B.C. and N.S. wrote the initial draft, and all authors reviewed and improved the manuscript.

SUPPLEMENTARY DATA

Supplementary data is available at *Zoological Journal of the Linnean Society* online.

CONFLICT OF INTEREST

Authors declare no conflict of interests.

FUNDING

G.B.C., E.S.-L., B.F.M.F., T.G.D., D.O.B.J., and A.G.G. received funding from the UK Natural Environmental Research Council (NERC) Seabed Mining And Resilience To Experimental impact (SMARTEx) project (Grant Reference NE/T003537/1), and G.B.C., A.G.G., T.G.D., H.W., E.S.-L., and D.O.B.J. received funding from The Metals Company Inc. (TMC) through its subsidiary Nauru Ocean Resources Inc. (NORI). NORI holds exploration rights to the NORI-D contract area in the CCZ regulated by the International Seabed Authority and sponsored by the government of Nauru. M.V.K. received funding from the National Council for Scientific and Technological Development (CNPq #305274/2021-0) and the São Paulo Research Foundation (FAPESP, Processes #2014/01332-0 and #2021/06866-6). E.S.-L. received financial support from the Spanish Research State Agency (MCIN/AEI/10.13039/501100011033) and the European Union Next Generation EU/PRTR (grant agreement No RyC2023-043275-I). The funders had no influence on the data or interpretations presented in this paper.

DATA AVAILABILITY

All data are incorporated into the article and its online [Supporting Information](#), or accessible in public databases. Faunal annotations from imagery data used for estimating abundance are available as tables in the [Supporting Information](#). Sequences generated in this study are available in GenBank under the accession numbers PV826147–PV826149 (COI) and PV822267–PV822271 (28S). This article is registered in ZooBank under urn:lsid:zoobank.org:pub:15C4CC37-7A38-49E2-BAF8-B2B956FEF527.

REFERENCES

- Amon DJ, Ziegler AF, Dahlgren TG *et al.* Insights into the abundance and diversity of abyssal megafauna in a polymetallic-nodule region in the eastern Clarion-Clipperton Zone. *Scientific Reports* 2016;6:30492. <https://doi.org/10.1038/srep30492>
- Benzoni F, Arrigoni R, Stefani F *et al.* Phylogenetic position and taxonomy of *Cycloseris explanulata* and *C. wellsi* (Scleractinia: Fungiidae): lost mushroom corals find their way home. *Contributions to Zoology* 2012;81:125–46. <https://doi.org/10.1163/18759866-08103001>
- Bitner MA, Melnik VP, Zezina ON. New paedomorphic brachiopods from the abyssal zone of the north-eastern Pacific Ocean. *Zootaxa* 2013;3613:281–8. <https://doi.org/10.11646/zootaxa.3613.3.6>
- Bribiesca-Contreras G, Dahlgren TG, Amon DJ *et al.* Benthic megafauna of the western Clarion-Clipperton Zone, Pacific Ocean. *ZooKeys* 2022;1113:1–110. <https://doi.org/10.3897/zookeys.1113.82172>
- Cairns SD. The deep-water Scleractinia of the Caribbean and adjacent waters. *Studies on the Fauna of Curaçao and Other Caribbean Islands* 1979;57:1–341.

- Cairns SD. A revision of the shallow-water azooxanthellate Scleractinia of the western Atlantic. *Studies on the Fauna of Curacao and Other Caribbean Islands* 2000;75:1–240.
- Cairns SD. New abyssal Primnoidae (Anthozoa: Octocorallia) from the Clarion-Clipperton Fracture Zone, equatorial northeastern Pacific. *Marine Biodiversity* 2016;46:141–50. <https://doi.org/10.1007/s12526-015-0340-x>
- Cignoni P, Callieri M, Corsini M *et al.* MeshLab: an Open-Source Mesh Processing Tool. *Computing* 2008;1:129–36. <https://doi.org/10.2312/LocalChapterEvents/ItalChap/ItalianChapConf2008/129-136>
- Fedorov A, Beichel R, Kalpathy-Cramer J *et al.* 3D Slicer as an image computing platform for the Quantitative Imaging Network. *Magnetic Resonance Imaging* 2012;30:1323–41. <https://doi.org/10.1016/j.mri.2012.05.001>
- Fleming BFM, Simon-Lledó E, Benoist N *et al.* Seabed heterogeneity regulates megabenthic community patterns in abyssal nodule fields. *Elementa: Science of the Anthropocene* 2025;13. <https://doi.org/10.1525/elementa.2024.00049>
- Folmer O, Black M, Hoeh W *et al.* DNA primers for amplification of mitochondrial cytochrome c oxidase subunit I from diverse metazoan invertebrates. *Molecular Marine Biology and Biotechnology* 1994;3:294–9.
- Glover A, Dahlgren T, Wiklund H *et al.* An end-to-end DNA taxonomy methodology for benthic biodiversity survey in the Clarion-Clipperton Zone, Central Pacific Abyss. *Journal of Marine Science and Engineering* 2015;4:2. <https://doi.org/10.3390/jmse4010002>
- Grischenko AV, Gordon DP, Melnik VP. Bryozoa (Cyclostomata and Ctenostomata) from polymetallic nodules in the Russian exploration area, Clarion-Clipperton Fracture Zone, eastern Pacific Ocean—taxon novelty and implications of mining. *Zootaxa* 2018;4484:1–91. <https://doi.org/10.11646/zootaxa.4484.1.1>
- Grischenko AV, Gordon DP, Melnik VP. Bryozoa (Cheilostomata) from polymetallic nodules in the Russian exploration area, Clarion-Clipperton Fracture Zone, eastern Pacific Ocean—taxon novelty and characteristics as macro- and megafaunal elements. *Zootaxa* 2024;5440:1–147. <https://doi.org/10.11646/zootaxa.5440.1.1>
- Hebert PDN, Ratnasingham S, de Waard JR. Barcoding animal life: cytochrome c oxidase subunit 1 divergences among closely related species. *Proceedings of the Royal Society of London. Series B: Biological Sciences* 2003;270:S96–9. <https://doi.org/10.1098/rsbl.2003.0025>
- Hein JR, Koschinsky A, Kuhn T. Deep-ocean polymetallic nodules as a resource for critical materials. *Nature Reviews Earth & Environment* 2020;1:158–69. <https://doi.org/10.1038/s43017-020-0027-0>
- Hoeksema BW, Yeemin T. Late detachment conceals serial budding by the free-living coral *Fungia fungites* in the Inner Gulf of Thailand. *Coral Reefs* 2011;30:975–. <https://doi.org/10.1007/s00338-011-0784-9>
- Hoeksema BW, Cairns S. World List of Scleractinia. *Deltocyathus* Milne Edwards & Haime, 1848, 2025. <https://www.marinespecies.org/scleractinia> (18 March 2025, date last accessed).
- Hourigan T. NOAA Deep Sea Corals Research and Technology Program. Version 1.6 [Occurrence dataset], 2020. https://ipt-obis.gbif.us/resource?r=noaa_dsc_rtp.
- Huang D, Meier R, Todd PA *et al.* Slow mitochondrial COI sequence evolution at the base of the metazoan tree and its implications for DNA barcoding. *Journal of Molecular Evolution* 2008;66:167–74. <https://doi.org/10.1007/s00239-008-9069-5>
- Huelsenbeck JP, Ronquist F. MRBAYES: Bayesian inference of phylogenetic trees. *Bioinformatics* 2001;17:754–5.
- International Seabed Authority. Minerals: Polymetallic Nodules, 2024. <https://www.isa.org/im/exploration-contracts/polymetallic-nodules/> (11 December 2024, date last accessed).
- Jones DOB, Arias MB, Van Audenhaege L *et al.* Long-term impact and biological recovery in a deep-sea mining track. *Nature* 2025;642:112–8. <https://doi.org/10.1038/s41586-025-08921-3>
- Kaiser S, Smith CR, Arbizu PM. Editorial: Biodiversity of the Clarion Clipperton Fracture Zone. *Marine Biodiversity* 2017;47:259–64. <https://doi.org/10.1007/s12526-017-0733-0>
- Katoh K, Rozewicki J, Yamada KD. MAFFT online service: multiple sequence alignment, interactive sequence choice and visualization. *Briefings in Bioinformatics* 2019;20:1160–6. <https://doi.org/10.1093/bib/bbx108>
- Keller NB. Some new data on madreporarian corals of the genus *Deltocyathus*. *Trudy Instituta Okeanologii Akademii Nauk SSSR* 1982;117:47–58.
- Kersken D, Janussen D, Arbizu PM. Deep-sea glass sponges (Hexactinellida) from polymetallic nodule fields in the Clarion-Clipperton Fracture Zone (CCFZ), northeastern Pacific: Part II—Hexasterophora. *Marine Biodiversity* 2018a;49:947–87. <https://doi.org/10.1007/s12526-018-0880-y>
- Kersken D, Janussen D, Martínez Arbizu P. Deep-sea glass sponges (Hexactinellida) from polymetallic nodule fields in the Clarion-Clipperton Fracture Zone (CCFZ), northeastern Pacific: Part I—Amphidiscophora. *Marine Biodiversity* 2018b;48:545–73. <https://doi.org/10.1007/s12526-017-0727-y>
- Kimura M. A simple method for estimating evolutionary rates of base substitutions through comparative studies of nucleotide sequences. *Journal of Molecular Evolution* 1980;16:111–20.
- Kitahara MV. The azooxanthellate coral fauna of Brazil. *Bulletin of Marine Science* 2007;81:265–72.
- Kitahara MV, Cairns SD. A revision of the genus *Deltocyathus* Milne Edwards & Haime, 1848 (Scleractinia, Caryophylliidae) from New Caledonia, with the description of a new species. *Zoosystema* 2009;31:233–48. <https://doi.org/10.5252/z2009n2a2>
- Kitahara MV, Cairns SD. *Azooxanthellate Scleractinia (Cnidaria, Anthozoa) from New Caledonia, Tropical Deep-Sea Benthos*, 32. Paris: Publications Scientifiques du Muséum, 2021.
- Kitahara MV, Cairns SD, Stolarski J *et al.* Deltocyathiidae, an early-diverging family of Robust corals (Anthozoa, Scleractinia). *Zoologica Scripta* 2013;42:201–12. <https://doi.org/10.1111/j.1463-6409.2012.00575.x>
- Kumar S, Stecher G, Li M *et al.* MEGA X: Molecular Evolutionary Genetics Analysis across computing platforms. *Molecular Biology and Evolution* 2018;35:1547–9.
- Lanfear R, Frandsen PB, Wright AM *et al.* PartitionFinder 2: new methods for selecting partitioned models of evolution for molecular and morphological phylogenetic analyses. *Molecular Biology and Evolution* 2017;34:772–3. <https://doi.org/10.1093/molbev/msw260>
- Lim S-C, Wiklund H, Glover AG *et al.* A new genus and species of abyssal sponge commonly encrusting polymetallic nodules in the Clarion-Clipperton Zone, East Pacific Ocean. *Systematics and Biodiversity* 2017;15:507–19. <https://doi.org/10.1080/14772000.2017.1358218>
- Lim SC, Wiklund H, Bribiesca-Contreras G *et al.* Diversity and phylogeny of demosponge fauna in the abyssal nodule fields of the eastern Clarion-Clipperton Zone, Pacific Ocean. *Zoologica Scripta* 2024;53:880–905. <https://doi.org/10.1111/zsc.12683>
- Maté J. Ecological, genetic, and morphological differences among three *Pavona* (Cnidaria: Anthozoa) species from the Pacific coast of Panama. *Marine Biology* 2003;142:427–40. <https://doi.org/10.1007/s00227-002-0956-9>
- McClain CR. The commonness of rarity in a deep-sea taxon. *Oikos* 2021;130:863–78. <https://doi.org/10.1111/oik.07602>
- McFadden CS, van Ofwegen LP. Stoloniferous octocorals (Anthozoa, Octocorallia) from South Africa, with descriptions of a new family of Alcyonacea, a new genus of Clavulariidae, and a new species of *Cornularia* (Cornulariidae). *Invertebrate Systematics* 2012;26:331. <https://doi.org/10.1071/is12035>
- Mejía-Saenz A, Simon-Lledó E, Partridge LS *et al.* Rock outcrops enhance abyssal benthic biodiversity. *Deep Sea Research Part I: Oceanographic Research Papers* 2023;195:103999. <https://doi.org/10.1016/j.dsr.2023.103999>
- Edwards M, Haime H. J. Recherches sur les polypiers. Mémoire 2. Monographie des turbinolides. *Annales des Sciences Naturelles, Zoologie, Series 3* 1848;9:211–344.
- Molodtsova TN, Opresko DM. Black corals (Anthozoa: Antipatharia) of the Clarion-Clipperton Fracture Zone. *Marine Biodiversity* 2017;47:349–65. <https://doi.org/10.1007/s12526-017-0659-6>
- OBIS. Ocean Biodiversity Information System. Intergovernmental Oceanographic Commission of UNESCO, 2025. <https://obis.org> (8 January 2025, date last accessed).

- Rabone M, Wiethase JH, Simon-Lledó E *et al.* How many metazoan species live in the world's largest mineral exploration region? *Current Biology* 2023;**33**:2383–96 e5. <https://doi.org/10.1016/j.cub.2023.04.052>
- Shearer TL, Coffroth MA. DNA BARCODING: Barcoding corals: limited by interspecific divergence, not intraspecific variation. *Molecular Ecology Resources* 2008;**8**:247–55. <https://doi.org/10.1111/j.1471-8286.2007.01996.x>
- Simon-Lledó E, Thompson S, Yool A *et al.* Preliminary observations of the abyssal megafauna of Kiribati. *Frontiers in Marine Science* 2019a;**6**:6. <https://doi.org/10.3389/fmars.2019.00605>
- Simon-Lledó E, Bett BJ, Huvenne VAI *et al.* Megafaunal variation in the abyssal landscape of the Clarion Clipperton Zone. *Progress in Oceanography* 2019b;**170**:119–33. <https://doi.org/10.1016/j.pocean.2018.11.003>
- Simon-Lledó E, Amon DBC, Guadalupe Cuvelier D *et al.* Abyssal Pacific Seafloor Megafauna Atlas. Version 1.0. [Standard]. Zenodo. <https://doi.org/10.5281/zenodo.8172728>.
- Simon-Lledó E, Amon DJ, Bribiesca-Contreras G *et al.* Carbonate compensation depth drives abyssal biogeography in the northeast Pacific. *Nature Ecology & Evolution* 2023b;**7**:1388–97. <https://doi.org/10.1038/s41559-023-02122-9>
- Simon-Lledó E, Baselga A, Gómez-Rodríguez C *et al.* Marked variability in distance-decay patterns suggests contrasting dispersal ability in abyssal taxa. *Global Ecology and Biogeography* 2025;**34**: <https://doi.org/10.1111/geb.13956>
- Stamatakis A. RAxML-VI-HPC: maximum likelihood-based phylogenetic analyses with thousands of taxa and mixed models. *Bioinformatics* 2006;**22**:2688–90. <https://doi.org/10.1093/bioinformatics/btl446>
- Taboada S, Riesgo A, Wiklund H *et al.* Implications of population connectivity studies for the design of marine protected areas in the deep sea: an example of a demosponge from the Clarion-Clipperton Zone. *Molecular Ecology* 2018;**27**:4657–79. <https://doi.org/10.1111/mec.14888>
- Todd PA. Morphological plasticity in scleractinian corals. *Biological Reviews of the Cambridge Philosophical Society* 2008;**83**:315–37. <https://doi.org/10.1111/j.1469-185x.2008.00045.x>
- Uhlenkott K, Simon-Lledó E, Vink A *et al.* Megafauna Morphotypes Annotated on Deep See Images in the German Contract Area for Polymetallic Nodule Mining, Clarion Clipperton Fracture Zone, Pacific [dataset]. PANGAEA – Data Publisher for Earth & Environmental Science, 2022. <https://doi.org/10.1594/PANGAEA.946800>
- Uhlenkott K, Simon-Lledó E, Vink A *et al.* Habitat heterogeneity enhances megafaunal biodiversity at bathymetric elevations in the Clarion Clipperton Fracture Zone. *Marine Biodiversity* 2023;**53**:1–13. <https://doi.org/10.1007/s12526-023-01346-z>
- Washburn TW, Jones DOB, Wei C-L *et al.* Environmental heterogeneity throughout the Clarion-Clipperton zone and the potential representativity of the APEI network. *Frontiers in Marine Science* 2021;**8**: <https://doi.org/10.3389/fmars.2021.661685>
- Wedding LM, Friedlander AM, Kittinger JN *et al.* From principles to practice: a spatial approach to systematic conservation planning in the deep sea. *Proceedings of the Royal Society B: Biological Sciences* 2013;**280**:20131684– <https://doi.org/10.1098/rspb.2013.1684>
- Wells JW. Notes on Indo-Pacific scleractinian corals. Part 10. Late Pleistocene ahermatypic corals from Vanuatu. *Pacific Science* 1984;**38**:205–19.